Металлофиз. новейшие технол. / *Metallofiz. Noveishie Tekhnol.*
2018, т. 40, № 3, сс. 411–421 / DOI: 10.15407/mfint.40.03.0411
Оттиски доступны непосредственно от издателя
Фотокопирование разрешено только
в соответствии с лицензией

© 2018 ИМФ (Институт металлофизики
им. Г. В. Курдюмова НАН Украины)

Напечатано в Украине.

PHYSICAL AND TECHNICAL BASIS OF EXPERIMENT AND DIAGNOSTICS

PACS numbers: 46.40.Cd, 61.43.Gt, 62.20.D-, 62.30.+d, 68.37.Tj, 81.05.Rm, 81.70.Cv

Characterization of Single SAW Velocities of Ti–6Al–4V Alloy as a Function of Porosity by SAM Simulation for Applications

Y. Al-Sayad, Z. Hadjoub, and A. Doghmane

Badji Mokhtar University
Laboratory of Semiconductors, Department of Physics, Faculty of Sciences, BO 12, CP 23000 Annaba, Algeria

Rayleigh wave modes depend on porosity of Ti–6Al–4V alloy with porosities between 60–75%. It is very important in many applications and understanding of bonding arrangements at propagating surface acoustic-wave velocities. These velocities are deduced from the analysis of the topped acoustic signatures' curves obtained by recording the output signal V. We used simulation of acoustic microscopy to measure Rayleigh velocities. The acoustic parameters were determined as follow: longitudinal (V_L), transverse (V_T), and Rayleigh (V_R) velocities from 1139 ms^{-1} to 285 ms^{-1}, from 87 ms^{-1} to 143 ms^{-1}, and from 562 ms^{-1} to 136 ms^{-1}, respectively, for porosity from 60% to 75%.

Key words: Ti–6Al–4V alloy, Rayleigh velocities, scanning acoustic microscopy (SAM), Young's modulus, surface acoustic waves (SAW) simulation.

Режими Релейових хвиль залежать від пористости стопу Ti–6Al–4V, яка становить 60–75%. Це дуже важливо для багатьох застосувань і розуміння сполучних пристроїв при поширенні поверхневих акустичних хвиль. Швидкості визначалися за допомогою аналізи усічених кривих акустичних характеристик, одержаних шляхом реєстрації вихідного сиґналу V. Моделюванням поверхневих акустичних хвиль вимірювалися Релейові швидкості. Визначено акустичні параметри: поздовжні (V_L), поперечні (V_T) швидкості та швидкість Релея (V_R) — від 1139 $мс^{-1}$ до 285 $мс^{-1}$, від 87 $мс^{-1}$ до 143 $мс^{-1}$ та від 562 $мс^{-1}$ до 136 $мс^{-1}$ відповідно (при пористості від 60% до 75%).

Corresponding author: Y. Al-Sayad
E-mail: yahya_sayaad@yahoo.com

Citation: Y. Al-Sayad, Z. Hadjoub, and A. Doghmane, Characterization of Single SAW Velocities of Ti–6Al–4V Alloy as a Function of Porosity by SAM Simulation for Applications, *Metallofiz. Noveishie Tekhnol.*, **40**, No. 3: 411–421 (2018), DOI: 10.15407/mfint.40.03.0411.

Ключові слова: стоп Ti–6Al–4V, Релейова швидкість, акустична мікроскопія, модуль Юнґа, моделювання поверхневих акустичних хвиль.

Режимы волн Рэлея зависят от пористости сплава Ti–6Al–4V, которая составляет 60–75%. Это очень важно для многих приложений и понимания связующих устройств при распространении поверхностных акустических волн. Скорости определялись с помощью анализа усечённых кривых акустических характеристик, полученных путём регистрации выходного сигнала V. Моделированием поверхностных акустических волн измерялись скорости Рэлея. Определены акустические параметры: продольные (V_L), поперечные (V_T) скорости и скорость Рэлея (V_R) — от 1139 мс$^{-1}$ до 285 мс$^{-1}$, от 87 мс$^{-1}$ до 143 мс$^{-1}$ и от 562 мс$^{-1}$ до 136 мс$^{-1}$ соответственно (при пористости от 60% до 75%).

Ключевые слова: сплав Ti–6Al–4V, скорость Рэлея, акустическая микроскопия, модуль Юнга, моделирование поверхностных акустических волн.

(Received November 24, 2017)

1. INTRODUCTION

1.1. Materials and Background

The mineralogist and chemist, William Gregor in 1791, first discovered titanium. Four years later, Martin Klaproth, based on the story of the Greek mythological children, the Titans, named the element as titanium. After that, more than 100 years were necessary to isolate the titanium metal from its oxide. Finally, the first alloys, as well as the popular Ti–6Al–4V alloy, were developed in the late 1940. The Ti–6Al–4V alloy is the most common used alloy among the commercially available titanium alloys. The reason for this success is the good balance of its properties and the intensive development and testing of this alloy during the approximately last 60 years [1]. In the present work, the behaviour of Ti–6Al–4V components fabricated by the using several process techniques is investigated in details. Experiments were conducted in a challenge to determine the influence of critical features such as surface quality porosity on the behaviour of Ti–6Al–4V alloy [2]. In order to identify mechanism, detailed examination of the changes of dynamic SAW velocities for vary application was carried out. In a second step, different porosities, as they seem to us, change dynamics of different elasticity-moduli values and type of surface acoustic waves' values. Configurations are described in terms of acoustic wave velocities (AWV) to understand the influence of porosities on mechanical properties of Ti6Al4V alloy by using process techniques to fabricate porous to reduce porosity. Porous Ti–6Al–4V alloy materials are used successfully with porosities' ranges from 60% to 75% under

compaction pressures in the range from 100 to 450 MPa. Ti–6Al–4V foam is produced by Space Holder Technique in powder metallurgy at temperature 1080°C with particle size of 400 μm [3]. Ti–6Al–4V alloy powders of less than 78 μm size with a nominal size of 58 μm were used in the experiments. The powders were irregular in shape and conform to ASTM 1580-01. As a space holder material, carbamide, also named urea, was chosen due to its advantages of shape and ease of removal prior to sintering spherical carbamide particles sieved to the size range of 0.6–1.0 mm.

2. THEORETICAL DETAILS

2.1. Determination of Acoustic Wave Velocities (AWV)

Rayleigh waves are a type of elastic surface wave that propagate on solids. They are also produced in materials by acoustic transducers, and are used in non-destructive testing for detecting defects. They are confined to within the wavelength or so of the surface, along which they propagate. They are also distinct from longitudinal and shear bulk acoustic waves (BAW) modes, which propagate independently at different velocities. In Rayleigh waves, there is a superposition of longitudinal and shear motions, which are intimately coupled, and they propagate together at a common velocity V_R [4]. Study of surface acoustic waves started back in 1887 when Lord Rayleigh first proposed [5] their existence. Surface acoustic waves (SAW) are modes of propagation of elastic energy along the surface of a solid, whose displacement amplitudes undergo exponential decay beneath this surface. Typically, almost all energy is localised within the depth of two wavelengths. Interest in surface acoustic waves has grown since Rayleigh's discovery. The many device applications utilising ultrasonics lead to a resurgence of interest in surface acoustic waves in the late 1960s, including ultrasonic detection of surface flaws [6] and ultrasonic delay lines [7]. Early transducer devices utilising SAWs on piezoelectric crystals [8] emerged around the same time, whilst theoretical considerations of the surface wave problem to include piezoelectric effects was firstly studied by Tseng [9, 10]. Further interest resulted from the multitude of signal processing applications available utilizing surface acoustic waves partly because the character of the wave can be changed in transit [11] as well as the fact the wave can be guided [12, 13] and even amplified [14].

In this study, the acoustic wave velocities (AWV) are studied. Using Scanning Acoustic Microscopy (SAM) simulation, different velocity values will be calculated when impacted to porosity on these velocities. That allows us to make use of them as possibility as making them in the engineering and architectural and medical applications.

2.2. SAM Principle

Scanning Acoustic Microscopy is a non-invasive imaging technique is based on ultrasound with assets of a similar resolution as having the light microscopy [15]. It studies dynamics to measure acoustic wave velocities (AWV) by SAM devices widely used in this study a frequency due to their stability. SAM is a non-destructive analytical tool for mechanical properties' investigations of bulk materials as well as alloys [16] that is the known dispersion behaviour of the dependence of the surface acoustic wave. According to SAW, velocity values in alloys' structures show us multiphenomena as Rayleigh velocity and elastic properties. However, let us appear the work principle of SAM. The simulations were carried out in the case of SAM under the following conditions: half-lens opening angle $\theta_n = 50°$, frequency $f = 140$ MHz, and properties of coupling liquid Freon whose density, $\rho = 1570$ Kg/m^3, and longitudinal velocity of liquid, $V_{liq} = 716$ m·s^{-1}, are summarised in tables below as well as different substrates with several porosities of Ti–6Al–4V alloy [17] (Fig. 1). Appearing SAM at the work principle is considered for specific mode detection.

3. RESULTS AND DISCUSSION

3.1. Fast Fourier Curves

The most important that was studied is scanning acoustic microscopy technique when acoustic waves downfall on material in the case these Ti–6Al–4V alloy materials through them coupling. Liquid as Freon, which properties have been cleared previously.

Acoustic waves work strikes material molecule mechanism move variety velocities, the most importantly, velocity is Rayleigh velocities

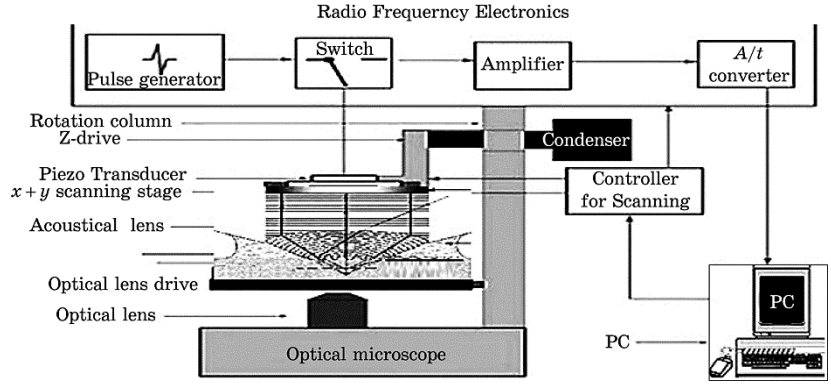

Fig. 1. Representation of a scanning acoustic microscope.

measured from through waves reflective from Ti–6Al–4V alloy materials to lens which is the image as energy outer is recorded as the output voltage $V(z)$, which sets following relationship [18]:

$$V(z) = \int R(\theta) P_2(\theta) e^{i2kz\cos\theta} \cos\theta \sin\theta d\theta, \quad (1)$$

where θ is the angle between a wave vector (**k**) and the lens axis (z), $P_2(\theta)$ is the lens pupil function, and $R(\theta)$ is the reflection function of the Ti–6Al–4V alloy material. This output voltage $V(z)$ depends on the distance (z) between lens and Ti–6Al–4V alloy material, which is reflective. As noted previously, reflective acoustic waves get overlap for these acoustic waves as a result of constructive and destructive interference between different propagating and treatment of periodic $V(z)$ curves by the fast Fourier transform (FFT). Rayleigh velocity (V_R) is determined from the principal peaks of the FFT *via* the following relationship [19]:

$$V_R = V_{\text{liq}} / \{1 - [1 - V_{\text{liq}}/(2f\Delta z)]^2\}^{1/2}, \quad (2)$$

where V_{liq} is the velocity in the coupling liquid, f is the operating frequency, and Δz is the period between two successive minima (or two successive maxima) in the $V(z)$ periodic response. The FFT peaks consist of valuable minor and values great the petition also. This one spectrum changes factors affecting in change arrangement of Ti–6Al–4V alloy materials in our study. They porosity are changed from atomic ranking to Ti–6Al–4V alloy materials increased porosity and note changes in interfered waves, which are reflected from Ti–6Al–4V alloy material clarified in spectra. However, this one change happened slowly when approaching porosity to up 75%. We can say that effect porosity to change characteristics of Ti–6Al–4V alloys from through molecules drift of the specimen and convergence for some, which shows Rayleigh velocities and is referred by pointer. In Figure 2, Rayleigh velocities change, whenever changed porous Ti–6Al–4V alloys will recognize as a function of porosity.

3.2. Elastic Moduli

Mechanical properties such as Young's modulus (E) determined from curves of porous Ti–6Al–4V alloys [3] are presented in Table 1 for samples containing minimum and maximum amount of porosities. As expected, mechanical properties of porous Ti–6Al–4V samples are better than the porous titanium samples in the same porosity range. In this study, elastic properties of materials with density $\rho = 4430$ kg/m^3 and Poisson ratio, $\nu = 0.325$ [3], can be expressed in terms of independent parameters, shear modulus (G), bulk modulus (B) [20], and

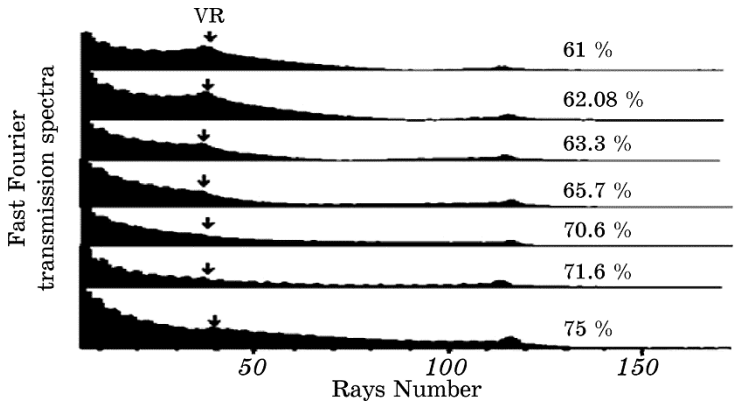

Fig. 2. FFT spectra with rays number of Ti–6Al–4V alloys at different porosities.

Young's modulus, as follow:

$$G = E/[2(\nu + 1)], \tag{3}$$

$$B = EG/[3(3G - E)], \tag{4}$$

$$V_L = V_T[(E - 4G)/(E - 3G)]^{1/2}, \tag{5}$$

$$V_T = \sqrt{G/\rho}\ , \tag{6}$$

for several porosities as in Table 1. Differences in porosity characteristics and the number contacts formed before and during porosity may be the reason of revealed difference. As higher porosity contribute to the decrease in elastic moduli of Ti–6Al–4V alloys, and for porosity increase, elastic moduli decrease occurs. This effect is more evident in

TABLE 1. Young's modulus, shear modulus, and bulk modulus values for minimum and maximum porosities of Ti–6Al–4V alloys.

Porosity, %	Experimental			Calculated	
	ρ, kg/m^3	E, GPa	ν	B, GPa	G, GPa
61	4430	3.8	0.325	4	1.4
62.08		3.55		3.38	1.34
63.3		2		1.86	0.74
65.7		1.1		1.1	0.42
70.6		0.6		0.6	0.23
71.6		0.50		0.5	0.19
75		0.25		0.24	0.09
75.3		0.23		0.22	0.087

porosity of Ti–6Al–4V alloys having elastic moduli values by 75.3% lower than that of ones in the same porosity range.

3.3. Measurable Acoustic Velocities of Ti–6Al–4V Alloys as a Function of Porosity

The treatment resulting fast Fourier transform (FFT) from the use of scanning acoustic microscopy simulation software to a conclusion Rayleigh velocities V_R, which is characterized by a large spectrum consisting of one wide peaks (Fig. 2), by measuring the output response V, following relationship (2). The peak consistent to the Rayleigh mode appears for all porosities 60% to 75%. The magnitude of V_R peaks is declining with increase of the porosities of Ti–6Al–4V alloys after calculation of reflection coefficient, $R(\theta)$, and acoustic material, $V(z)$, the characteristics of highly porous materials is agreed with same low velocity values *via* clearly Table 2. We were able to deduce the dependence of Rayleigh velocities, V_R, of Ti–6Al–4V alloys. After FFT analysis leads to the calculation of longitudinal (V_L) and transversal (V_T) values by Eq. (5) and (6) as in Table 2; such high values are impossible to characterize this material with effective porosities creation use of former relations between SAW velocity and porosity. To verify this relation, it is necessary to select the best slower velocity than well-investigated material to application. Relationship between longitudinal velocities, transverse velocities, and Rayleigh velocities with low porosities of Ti–6Al–4V alloys for application due to possible change of physical alloys and the relationship between the changed porosity due to creation methods applied. The quantification of the results *via* computer fitting all porosity of Ti–6Al–4V alloys in this part takes an exponential dependence:

TABLE 2. Calculated and experimental SAW velocity (V_R,V_L, and V_T) values for minimum and maximum porosities of Ti–6Al–4V alloys.

Porosity, %	Experimental			Calculated	
	ρ, kg/m^3	ν	V_R, m/s	V_L, m/s	V_T, m/s
61	4430	0.325	3.8	1139	557
62.08			3.55	1080	550
63.3			2	802	409
65.7			1.1	612	308
70.6			0.6	452	228
71.6			0.50	412	207
75			0.25	285	143
75.3			0.23	275	140

$$\text{SAW velocities (m/s)} = V_0 + \beta e^{-1/R_0(\text{Porosity},\%)}, \quad (7)$$

where the relationship between porosities and surface acoustic wave velocities of Ti–6Al–4V alloys are expositional function $V = V_0 + \beta e^{-1/R_0}$ [m/s] of porosity [%]. $V_0 = V_{L0}$,V_{T0}, or V_{R0}, and β are parameters of the Exp. Dec. curve fit model and R^2 is regression line. V is the velocities of the porous material. Dynamic method was used to determine the SAW velocities of Ti–6Al–4V alloys. The best fitting curves for SAW velocities' data of samples in the present study give Eq. (7) for Ti–6Al–4V alloy samples. We can give general form equation to understand the relation porosity 60% to 75% with SAW velocities as Eq. (7).

It is clear that the linear dependence is obtained in all cases for slope changes with every kind of SAW velocity curves (Fig. 3). In studies, variation of relative mechanical property with small porosity (P, %) of samples has been shown to obey the relation. Use of porosity content as a single variable in determining the properties may lead to misleading results in mechanical property calculations since samples having similar porosity levels may have different interparticle-bond state. SAW

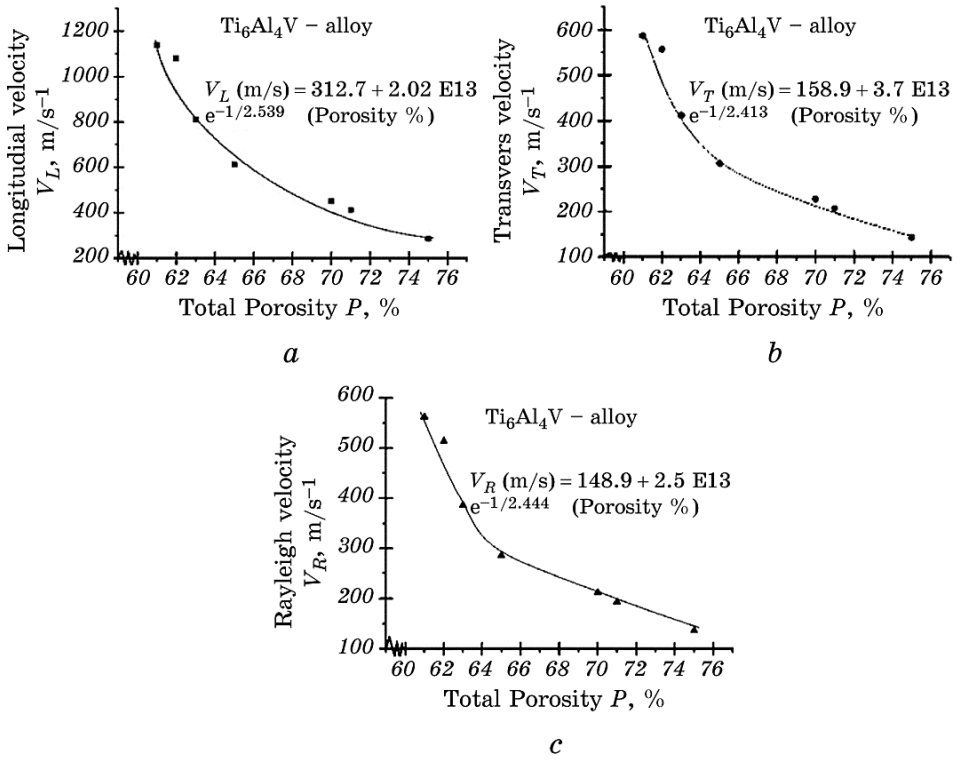

Fig. 3. Effects of porosities of Ti–6Al–4V alloys on longitudinal velocities V_L (■) (*a*), transverse velocities V_T (●) (*b*), and Rayleigh velocities V_R (▲) (*c*).

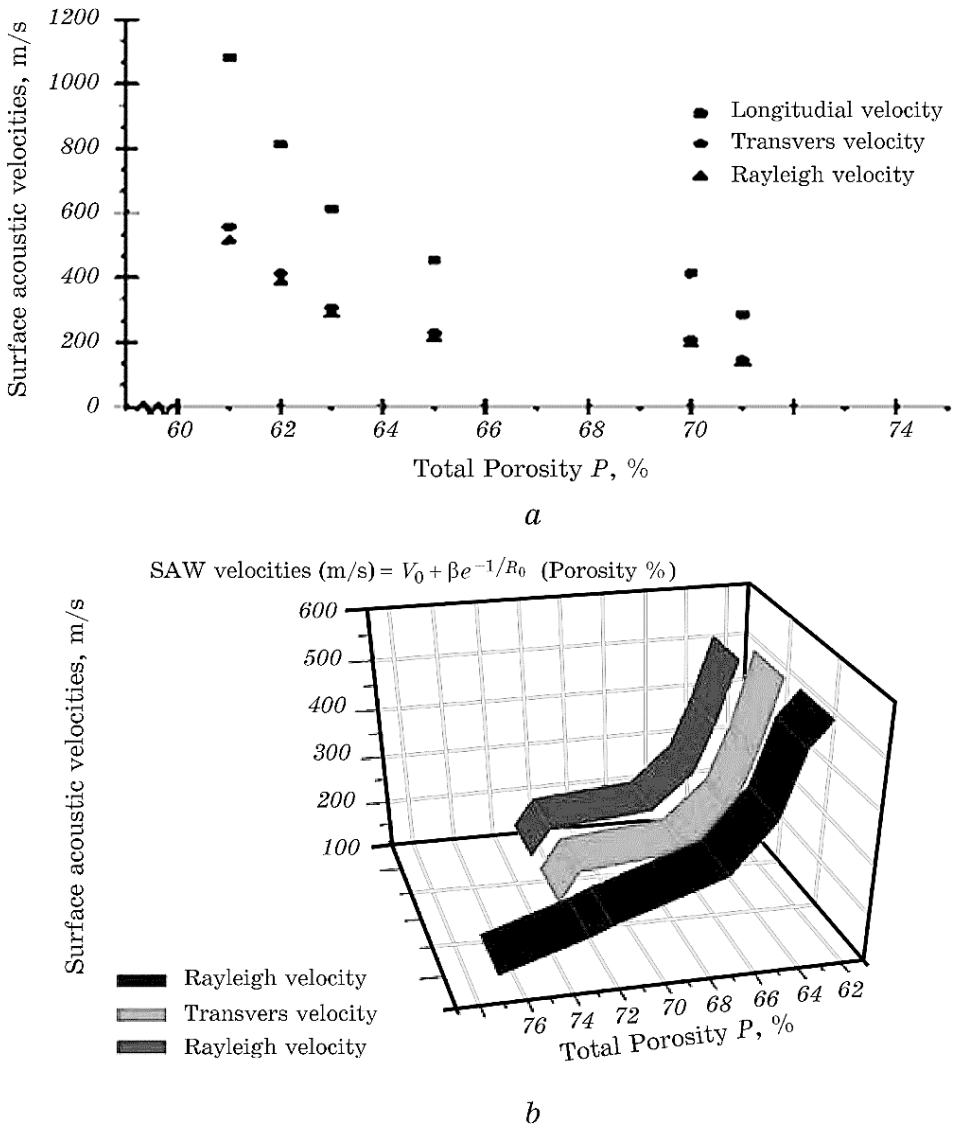

Fig. 4. SAW velocities of Ti–6Al–4V alloys as a function of porosity. SAW velocities, V_L, V_T, V_T, in different presentations (*a*) and (*b*).

velocities of Ti–6Al–4V alloys as a function of porosity are shown in Fig. 4.

4. CONCLUSIONS

Every single change in the peak of FFT spectra of Ti–6Al–4V alloys

subsequent from a change structures organizer is due to changed porosity applied. The change in the value of porosity of Ti–6Al–4V alloys influence the elastic moduli (E, B, G) such as SAW velocity (V_L, V_T, V_R) were realized.

Increasing porosity of Ti–6Al–4V alloys (61% to 75.3%) as experimental and calculated material leads to a decrease of elastic moduli, E, G, B, as from 3.8 to 0.23 GPa, from 4 to 0.22 GPa, and from 1.4.8 to 0.087 GPa, respectively.

These results show the dependence of the curve divergence of the period velocity characterized with a physical understanding of type of bonding molecules' arrangements in materials.

The rank of this analysis is in the determination, for a given SAW velocity of known porosities of Ti–6Al–4V alloys, of favourite trial about Rayleigh modes for porous 60% to 75%.

Decreasing porosities of Ti–6Al–4V alloys round (from 61% to 75.3%) pointers to increasing affected on each change in the V_L (■), V_T (●), and V_R (▲) values as follow: from 1139 ms^{-1} to 285 ms^{-1}, from 587 ms^{-1} to 143 ms^{-1}, and from 562 ms^{-1} to 136 ms^{-1}, respectively. Finally, SAW velocities (longitudinal, transverse, Rayleigh ones) were found to be dependent on porosities of Ti–6Al–4V alloys line by means of the general formula being the kind of exponential function as follows: SAW velocities (m/s) $= V_0 + \beta e^{-1/R_0}$ (porosity, %), R^2 is regression line.

REFERENCES

1. M. Peters, H. Hemptenmacher, J. Kumpfert, and C. Leyens, *Titanium and Titanium Alloys* (Eds. C. Leyens and M. Peters) (Weinheim: Wiley-VCH: 2003).
2. G. Kotan and A. Sëakir Bor, *Turkish J. Eng. Env. Sci.*, **31**: 149 (2007).
3. Sh. R. Bhattarai, Kh. A.-R. Khalil, M. Dewidar, P. H. Hwang, H. K. Yi, and H. Y. Kim, *J. Biomedical Materials Research Part A*, **86A**, Iss. 2: 289 (2008).
4. A. Briggs, *Acoustic Microscopy* (Oxford: Clarendon Press: 1992).
5. J. David and N. Cheeke, *Fundamentals and Applications of Ultrasonic* (Boca Raton: CRC Press: 2002).
6. I. A. Viktorov, *Rayleigh and Love Waves. Section 1.1* (New York: Plenum: 1967).
7. J. E. May, *IEEE Spectrum*, **2**: 73 (1965).
8. R. M. White and F. W. Voltmer, *Appl. Phys. Lett.*, **7**: 314 (1965).
9. C.-C. Tseng, *J. Appl. Phys.*, **38**: 4281 (1967).
10. C.-C. Tseng, *J. Appl. Phys.*, **41**: 2270 (1970).
11. R. M. White, *IEEE Trans. Elect. Dev.*, **ED14**: 181 (1967).
12. H. F. Tiersten, *J. Appl. Phys.*, **40**: 770 (1969).
13. D. L. White, *IEEE Ultrasonics Symp.* (Vancouver: 1967).
14. E. Stern, *Lincoln Lab. Tech.*, Note No. 1968-36, M.I.T. (1968).
15. J. B. Liu, J. N. Peterson, F. Forsberg, M. D. Jaeger, D. B. Kynor, and R. J. Kline-Schoder, *Ultrasonics*, **42**: 337 (2004).

16. S. Bouhedja, I. Hadjoub, A. Doghmane, and Z. Hadjoub, *phys. status solidi (a)*, **202**: 1025 (2005).
17. K. Wang, *Mat. Sci. Eng. A*, **213**: 134 (1996).
18. C. G. R. Sheppard and T. Wilson, *Appl. Phys. Lett.*, **38**: 858 (1981).
19. J. Kushibiki and N. Chubachi, *IEEE Sonics Ultrason.*, **SU-32**, No. 2, 189 (1985).
20. R. G. Munro and J. Res, *Nat. Inst. Stand. Technol.*, **105**: 709 (2000).